Transactions, SMiRT-25
Charlotte, NC, USA, August 4-9, 2019
Division V (Modelling, Testing and Response Analysis of Structures, Systems and Components)

NUMERICAL ISSUES IN DEVELOPING IN-STRUCTURE RESPONSE SPECTRA FOR SEISMICALLY ISOLATED NUCLEAR STRUCTURES

Manish Kumar[1*†] and Andrew S. Whittaker[2]

[1]*Department of Civil Engineering, Indian Institute of Technology Bombay, Mumbai, India*
[2]*Department of Civil, Structural and Environmental Engineering, University at Buffalo, NY, U.S.A.*

SUMMARY

Seismic isolation of a nuclear power plant (NPP) significantly reduces seismic demands in structural elements and nonstructural systems and components in the horizontal plane but may amplify demands in the vertical direction, depending on the frequency content of the ground motion and the mechanical properties of the isolation system. In-structure response spectra in a base-isolated NPP obtained using seismic response-history analysis, which are used for equipment qualification, are sensitive to the chosen numerical and modelling techniques, both of which are investigated in this paper. Three representations of base-isolated NPP are considered: 1) a two-node macro model, 2) a lumped-mass stick model, and 3) detailed finite element model. Two damping definitions and three modelling approaches are investigated. The results allow the reader to make informed decisions regarding selection of a numerical model and implementation of damping needed to obtain reliable floor response spectra for different intensities of earthquake shaking.

INTRODUCTION

Seismic isolation using low damping rubber (LDR), lead–rubber (LR) and Friction Pendulum bearings is a viable strategy for mitigating the effects of extreme earthquake shaking on safety-related nuclear structures. A series of studies have investigated the effect of design and beyond design earthquake shaking on base-isolated nuclear power plants (NPPs) (e.g., Kumar *et al.* (2015a), Kumar *et al.* (2015b), Kumar *et al.* (2015c), Kumar *et al.* (2015d), Kumar *et al.* (2014)) and formulated draft design guidance to achieve specific performance goals at the plant level. Key to equipment design and plant-level seismic risk calculations are robust estimates of in-structure floor acceleration response spectra. The ordinates of in-structure floor spectra are based on seismic response-history analysis of numerical models. Different NPP models and numerical techniques can be used, depending on the goals of the analysis and the response quantities required. The numerical response of a nonlinear system (e.g., soil, isolators, and superstructure) is especially sensitive to the definition of damping in the model. A number of researchers have identified issues associated with the estimation of numerical response of a viscously damped nonlinear system (e.g., Hall (2006), Charney (2008), Petrini *et al.* (2008)). A few remedies have been proposed (e.g., Léger and Dussault (1992), Jehel *et al.* (2014), Chopra and McKenna (2015)) but none address the unique challenges associated with the definition of damping in a base-isolated structure. Kelly (1999), Kelly and Marsico (2015), and Hall (1999) discuss the effect of damping on the response of a base-isolated structure but not the challenges associated with the specification of damping in a numerical model. Past research by the authors of this paper (Kumar and Whittaker (2018), Kumar *et al.* (2019)) has highlighted, but not quantified, the challenges, which has delayed the development of a solution. This paper investigates the effect of numerical modeling techniques, with focus on damping, on in-structure response spectra of base-isolated

*Correspondence to: Department of Civil Engineering, Indian Institute of Technology Bombay, Mumbai 400076, India
†E-mail: mkumar@iitb.ac.in

NPPs. Numerical challenges in the development of floor response spectra using different NPP model representations and associated damping options are discussed. Limitations of all models are highlighted and recommendations are provided for appropriate damping formulations in contemporary software programs. For final design, the authors advocate analysis of three-dimensional finite element models.

NUMERICAL MODEL

Base-isolated nuclear power plant

The three representations of a base-isolated NPP, shown in Figure 1, are considered here: 1) two-node macro (TNM) model, 2) lumped-mass stick (LMS) model, and 3) finite element (FE) model. The total mass of the NPP is 152,300 tons and basemat dimensions are 100m×60m×2.5m.

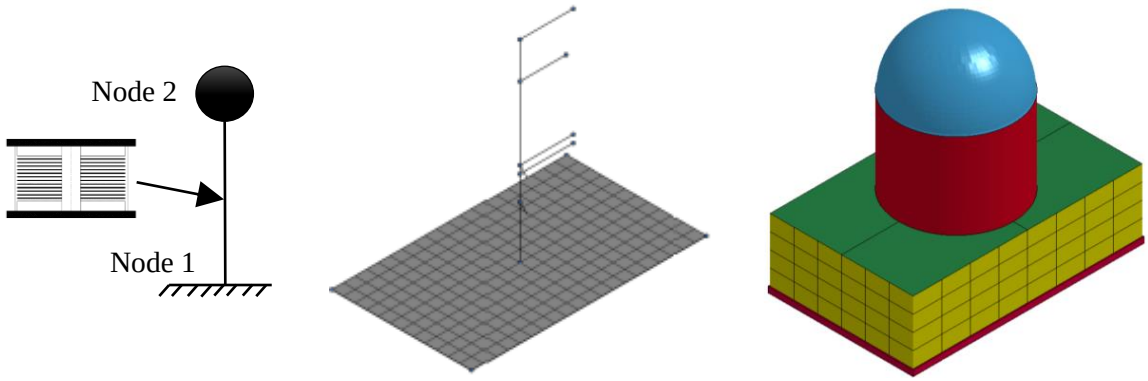

a) Two-node macro model b) Lumped mass stick model c) Finite element model

Figure 1. Modeling representation of nuclear power plants

The two-node macro model created in OpenSees is the most simplified representation of a base-isolated NPP amenable to large number of seismic response-history analyses. All six degrees of freedom of the bottom node (node 1) are fixed to the ground, as are the three rotational degrees of freedom at the top node. The two nodes are joined by the isolator element. The superstructure above the isolation interface is lumped as a rigid mass and all bearings of isolation system are assumed to respond equally. The static (gravity load) pressure on a single bearing is estimated by dividing the total weight of the superstructure by the number of bearings in the isolation system. The total weight is divided by g to obtain the equivalent mass M, which is lumped in the three translational directions at node 2 for static and dynamic analyses.

The stick model of the NPP is recreated in OpenSees (McKenna *et al.*, 2006) from EPRI (2007), which provides the equivalent nodal and element properties of the stick models created in SAP2000 (CSI, 2007). The three-dimensional model of NPP is simplified to three concentric lumped-mass stick models of the Coupled Auxiliary and Shield Building (ASB), Containment Internal Structure (CIS), and the Steel Containment Vessel (SCV). These three substructures constitute 86%, 11%, and 3% of the total mass of the NPP superstructure. The stick model of the NPP is isolated through a common basemat slab on LR bearings, as shown in Figure 2. A symmetric layout of 273 isolators is used beneath the basemat.

A FE model of the representative NPP described in Orr (2003) was created in LS-DYNA (LSTC, 2012). This NPP consists of an Auxiliary Building (AB), a Concrete Containment Vessel (CCV), and a Containment Internal Structure (CIS), all sharing a common basemat. The CIS is joined only to the basemat and the AB is joined to the CCV. The AB and CCV are modeled using shell elements, and the CIS and basemat are modelled using solid elements. Linear elastic properties for concrete and steel materials are assumed. The dimensions and sectional views of the NPP and the locations where responses are reported are shown in Figure 4. The NPP is isolated on a common basemat slab using a symmetrical layout of 273 LR bearings. The modal properties of the fixed base superstructure and base-isolated NPPs are presented in Table 1 and Table 2, respectively, for the three models. Detailed modal analysis of the three models and verification with other software is available in Kumar *et al.* (2015d) and Kumar and Whittaker (2018).

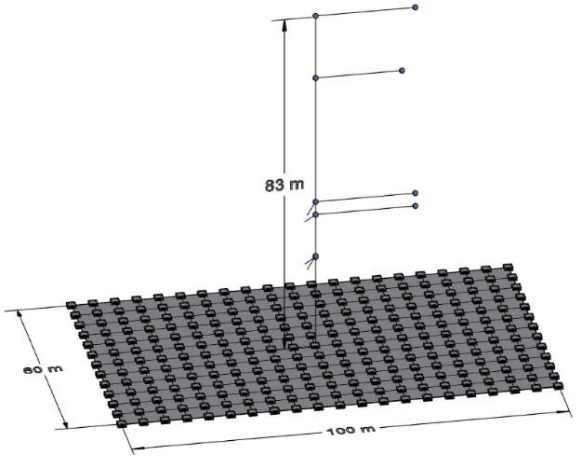

Figure 2. Lumped mass stick (LMS) model

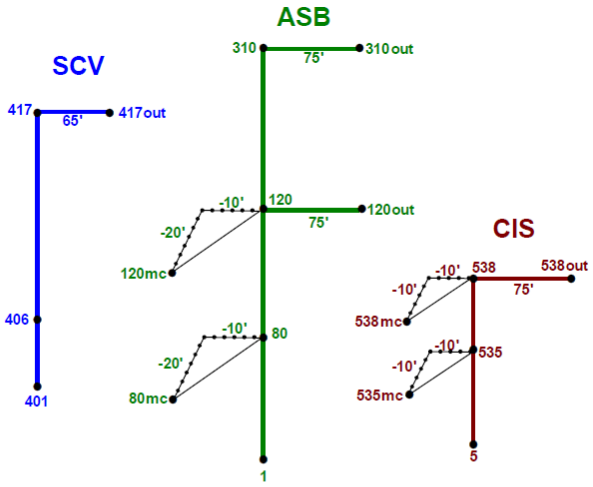

Figure 3. Components of the LMS model (EPRI, 2007)

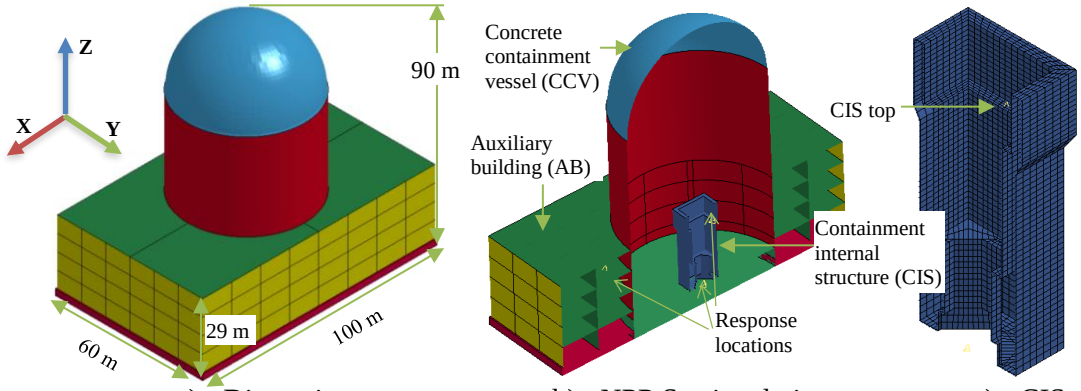

a) Dimension b) NPP Sectional view c) CIS

Figure 4. Finite element model of the archetype NPP

Table 1. Modal frequencies (Hz) of the superstructure

Model	LMS			FE	
	ASB	SCV	CIS	AB (ASB +SCV)	CIS
Horizontal 1	2.77	3.63	11.75	3.41	7.03
Horizontal 2	3.03	5.55	12.52	3.60	7.03
Vertical	9.61	16.2	40.07	8.96	14.53

Table 2. Modal frequencies (Hz) of the base-isolated NPP

	Method of calculation			
Direction	Theory	TNM	LMS	FE
Horizontal (post-elastic)	0.50	0.50	0.50	0.50
Vertical	18.87	--	--	--.
Rotation-plan	--	--	0.70	0.49

Isolation System

Analyses were performed for an isolation system with a time period, T, equal to 2 sec, and a ratio of characteristic strength to supported weight, Q_d/W, equal to 0.12. The selected design of the isolation system was dictated by the high seismic hazard at the Diablo Canyon NPP site, which is the assumed location of the base-isolated NPP analyzed in this paper. The geometric and mechanical properties of the LR bearings used for the analysis are summarized in Table 3. The procedure to obtain these properties is described in Kumar *et al.* (2015b) and not repeated here. In this table, a) the reported period, T, is that associated with the flexibility of the elastomer, and not the secant stiffness to expected maximum displacement, and b) the characteristic strength, Q_d, is normalized by the supported weight. The assumed bilinear hysteresis of the LR bearing is described in Figure 5.

Table 3. Geometrical and mechanical properties of elastomeric bearings (T = 2 s, Q_d/W = 0.12)

Property	Notation	Value
Single rubber layer thickness, mm	t_r	10
Number of rubber layers	n	27
Steel shim thickness, mm	t_s	4.76
Outer diameter, mm	D_o	1531
Lead core diameter, mm	D_i	314
Shear modulus, MPa	G	0.80
Bulk modulus of rubber, MPa	K_{bulk}	2000
Yield stress of lead, MPa	σ_L	8.5
Yield displacement, mm	u_y	21
Gravity pressure, MPa	p_{static}	3.0

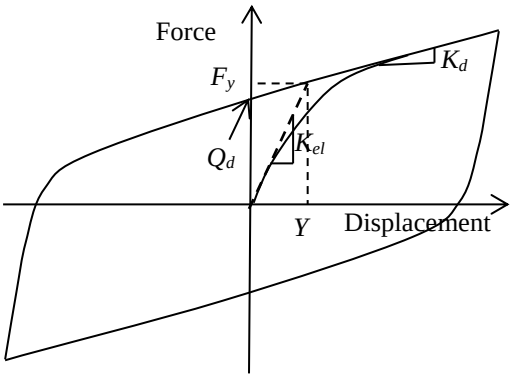

Figure 5. Mathematical model of a lead rubber bearing in the horizontal (shear) direction

SEISMIC HAZARD

The response-history analyses of the NPPs were performed using 30 sets of three-component ground motions selected and then spectrally matched to be consistent with uniform hazard response spectra (UHRS) for design-basis earthquake shaking at the site of the Diablo Canyon Nuclear Generating Station. The UHRS was calculated for a return period of 10,000 years. Complete details on the ground motions are presented in Kumar *et al.* (2015e). The 30 three-component sets of scaled ground motions were used to perform nonlinear response-history analysis and obtain response percentiles. One of ground motions (NGA-72, Lake Hughes, 1971 San Fernando earthquake) was used to generate response spectra at different locations and damping models. The 5% damped acceleration response spectra for this ground motion in the two horizontal directions and the vertical direction are shown in Figure 6.

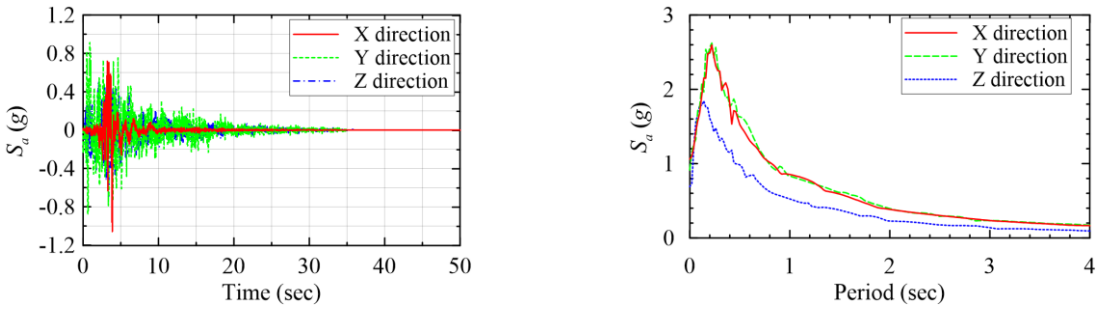

a) Acceleration histories b) Response spectra

Figure 6. Surface free-field acceleration histories and response spectra for the NGA-72 ground motion scaled to the DBE spectra, Diablo Canyon Nuclear Generating Station, site class B-C

DAMPING

Contemporary structural analysis tools (e.g., OpenSees and LS-DYNA) employ different schemes to model damping. The ordinates of the in-structure response of a base-isolated NPP are sensitive to the definition and value of damping used for the analysis (e.g., Kumar *et al.* (2015d)). In addition, the three models of the base-isolated NPP require different strategies to define appropriate damping to the components of the models to obtain consistent results for response-history analysis. Rayleigh damping is the most popular method of assigning viscous damping to a structural system. The effective Rayleigh damping ratio in the n^{th} mode of vibration is calculated as:

$$\xi_n = \frac{\alpha_M}{2\omega_n} + \frac{\beta_K}{2}\omega_n, \quad where \ \alpha_M = \frac{2\xi\omega_i\omega_j}{\omega_i + \omega_j}; \beta_K = \frac{2\xi}{\omega_i + \omega_j} \tag{1}$$

where ω_n is the angular frequency of the n^{th} mode, and ω_i and ω_j are the angular frequencies of the vibration modes to which a damping value (e.g., ξ = 2%) is assigned. Two special cases of Rayleigh damping are mass-proportional damping (β_K = 0) and stiffness-proportional damping (α_M = 0).

Ideally, an elastic concrete superstructure in an isolated NPP would be assigned a different damping ratio (e.g., 4%) than the supplementary viscous damping assigned to the LR bearings (e.g., 2%, in addition to its own hysteretic damping). The vibration modes that are of interest and primarily contributes to the response of base-isolated NPPs are: 1) horizontal and vertical response of the isolation system, and 2) first two horizontal modes of each of the superstructure components (CIS, AB/ASB, CCV/SCV). The frequency of these modes vary widely (0.5 Hz to 18.7 Hz) and the challenge is to assign damping to each component of the model, which is physically representative over entire range of response values. Two damping plots are presented in Figure 7 for the LMS model in OpenSees: 1) 2% damping based on horizontal isolation mode (*f*=0.5 Hz) and the vertical mode (*f*=18.7 Hz) of the isolation system, and 2) 4% damping based on first horizontal mode of the ASB (2.77 Hz) and the second horizontal mode of CIS (12.52 Hz). The Rayleigh damping assignment based on two modal frequencies cannot effectively capture appropriate damping in different components of the NPP. The damping based on first assignment, underdamps the superstructure modes, and the damping based on the second assignment severely overdamps the isolation modes. In addition, the damping assignment based on initial stiffness of the isolators will provide inaccurate estimate of the nonlinear response of the isolation system, unless the Rayleigh damping coefficients are updated at each analysis step (Charney, 2008).

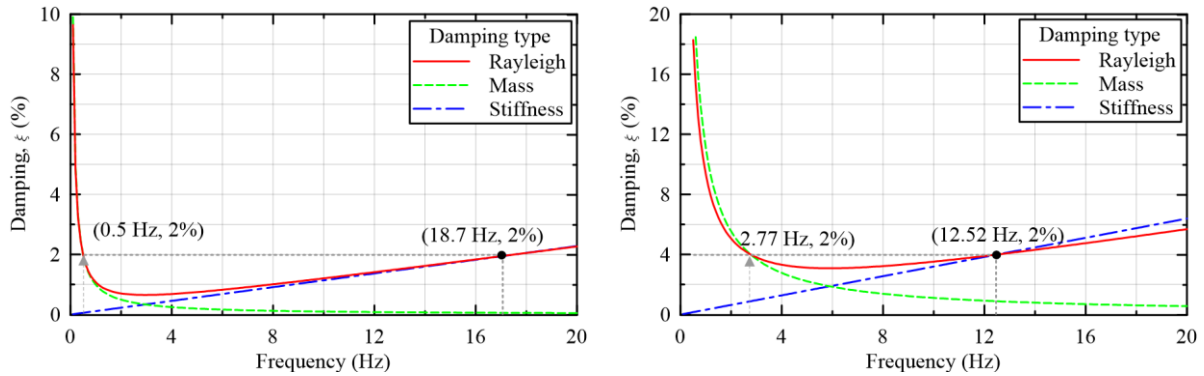

a) Isolator (2% isolation mode) b) Superstructure (4% horizontal modes)

Figure 7. Damping ratio versus frequency for three damping formulation and two modal assignments

Another popular method is to assign equal damping to a number of modes in a model. The limitation of this approach is that the same damping value must be defined to the first *n* number of modes. In addition, this is also based on initial stiffness and is not updated with time during ground motion shaking. One solution to the problem would be to not use equivalent viscous damping and obtain damping from the hysteretic energy dissipation. However, this will require that all elements be modeled as nonlinear, which may be computationally too expensive. The damping options available in contemporary software programs are investigated in the following sections.

OpenSees

OpenSees provides two options to include damping in a structural model: 1) Rayleigh damping, and 2) modal damping. Mass and stiffness proportional damping are modeled as special cases of Rayleigh damping. The general form of the Rayleigh damping in OpenSees is:

$$C = \alpha_M M + \beta_K K_t + \beta_{K0} K_0 + \beta_{Kc} K_c \quad (2)$$

where *C*, *M*, and *K* are the damping, mass and the stiffness matrices. The subscript *0*, *t*, and *c* refers to the initial, tangent (current), and committed state, respectively in the response-history analysis. This modal damping formulation has recently been implemented in OpenSees by Chopra and McKenna (2015). It

allows a damping ratio to be assigned to the first specified number of modes and has been shown to remove spurious damping-induced moments at joints. However, this method does not allow a different damping ratio to be assigned to the vibration modes of the isolation system and the superstructure. This limitation is addressed through the *region* command, which can be used to define different damping to ranges of nodes and elements. Five damping strategies, presented in Table 4, were investigated in OpenSees.

Table 4. Damping definitions used in OpenSees models

I	Modal	2% damping to the first *n* (=30, 50, 100) number of modes
II	Rayleigh	2% damping to horizontal and vertical isolation modes
III	Mass	2% damping to horizontal isolation modes
IV	Stiffness	2% damping to vertical isolation mode
V	Region	2% damping horizontal and vertical isolation modes + 4% damping to the first and second horizontal modes of the ASB and CIS, respectively

Two-Node Macro Model

The two-node macro model was assigned damping using the first four damping formulations described in Table 4. The numerical responses of the TNM model subject to the 30 ground motions are presented in Table 5. The in-structure response spectra in the three directions at the top node of the TNM model for the ground motion are presented in Figure 8.

Table 5. Mean peak in-structure response of the TNM model for different damping schemes

No.	Damping	Resultant acc. (*g*)	Resultant disp. (mm)	Zero period acceleration (*g*)			Spectral acceleration (*g*)		
				a_X	a_Y	aZ	S_{aX}	S_{aY}	S_{aZ}
I	Modal	0.34	234	0.28	0.29	4.25	1.03	0.97	18.57
II	Rayleigh	0.35	250	0.29	0.3	1.89	1.04	0.98	8.46
III	Mass	0.35	250	0.29	0.3	3.87	1.05	0.98	16.88
IV	Stiffness	0.37	263	0.29	0.32	1.89	1.05	0.98	8.45

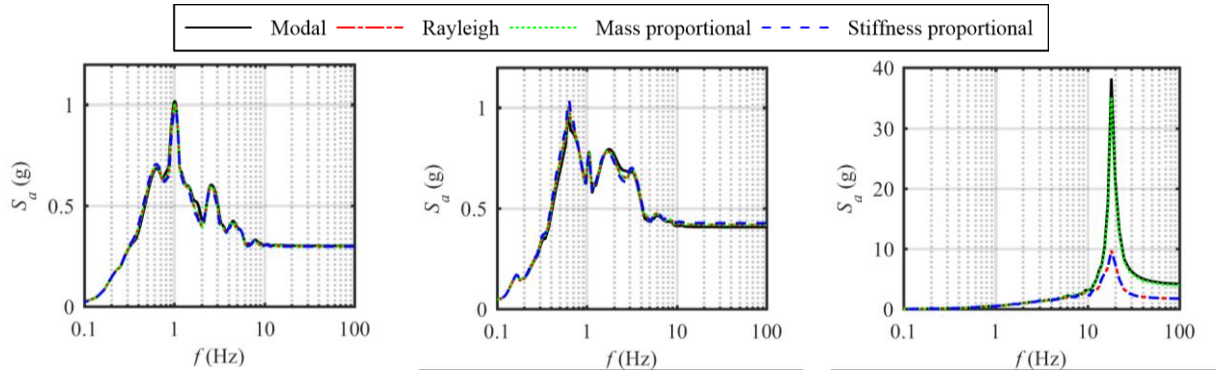

a) X direction b) Y direction c) Z direction

Figure 8. Response spectra at Node 2 of the two-node macro model

Modal damping provides the smallest estimate of the horizontal displacements. The Rayleigh and the mass proportional damping provide same damping to the isolation mode and hence the horizontal displacements are equal. The stiffness proportional damping based on the axial vibration mode results in a slightly greater horizontal displacement. Although the damping schemes provide near identical values of horizontal acceleration response, the vertical responses differ significantly. The large vertical accelerations associated with the modal and mass proportional damping formulations can be explained by their formulations in OpenSees. The TNM model has three mode shapes (2 horizontal and 1 axial) for the assumed boundary conditions. The modal analysis in OpenSees determines only the first (*n*-1) modal frequencies of an *n* DOF

model and so damping could not be assigned to the axial (3rd) mode using this option. The mass proportional damping based on the isolation frequency results in very small damping in the high frequency axial mode.

Lumped Mass Stick Model

All five damping formulations of Table 4 were investigated for the LMS model in OpenSees. The number of modes required for the modal damping formulation to capture in-structure response was assessed by developing response spectra at different locations in the building by assigning modal damping to the first 30, 50 and 100 modes. The frequencies for the 30th, 50th and 100th modes of the LMS model in OpenSees are 18.9 Hz, 31.2 Hz, and 62.9 Hz, respectively. Data are presented in Figure 9. No consistent trend was obtained for any locations and for the chosen range of frequencies (i.e., 0.1 Hz to 100 Hz). In general, the spectral accelerations were essentially identical for frequencies up to 1 Hz, but differed at higher frequencies as seen in the figure. (All subsequent analyses using the modal damping formulation were performed using first 100 modes.) Plots of in-structure response spectra are obtained for different locations in the LMS model using the first four damping formulations in Table 4 and are presented in Figure 10. There is significant difference between the horizontal spectral accelerations obtained using the four damping formulations, especially at frequencies between 1 and 10 Hz. All four damping formulations result in comparable spectral accelerations in the vertical direction, except for mass proportional damping that significantly overestimates it because the damping is tiny in the high frequency modes.

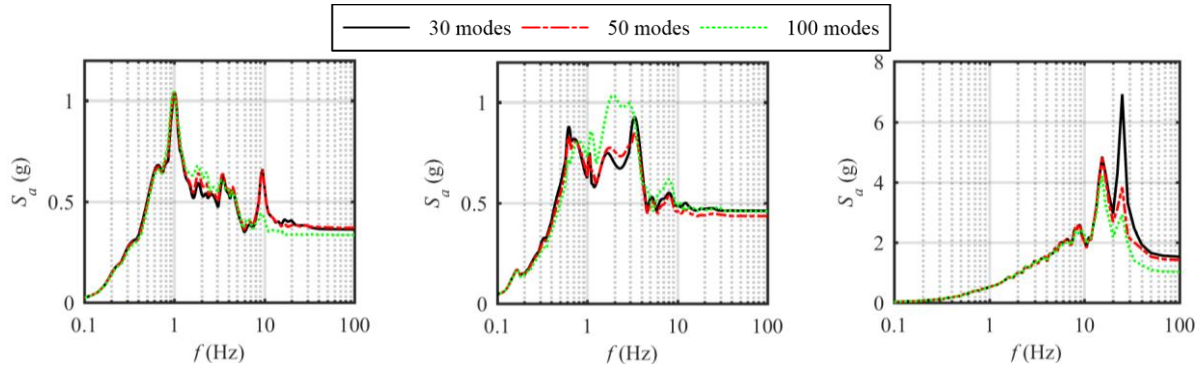

a) X direction b) Y direction c) Z direction

Figure 9. In-structure response spectra at the center of the basemat (2137) for modal damping

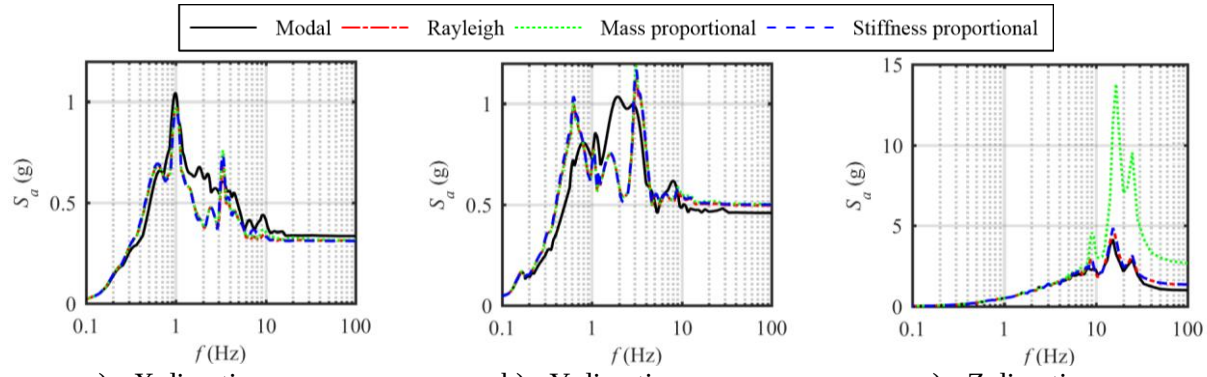

a) X direction b) Y direction c) Z direction

Figure 10. In-structure response spectra at the mid-height of the ASB (120)

Three damping options are investigated in more detail, including the *region* command through which damping values can be assigned to different ranges of nodes and elements. This option is especially useful for base-isolated structures owing to their widely spaced, but equally important, frequencies of interest. This option was used to assign different damping to isolators and the superstructure in the LMS model. The isolation system was assigned 2% damping based on the horizontal isolation frequency (0.5 *Hz*) and the

vertical frequency (18.7 *Hz*). The elastic superstructure was assigned Rayleigh damping of 4% based on first horizontal mode of ASB (2.8 Hz) and the second horizontal mode (12.5 *Hz*) of the superstructure. The plots of in-structure response spectra obtained using the three damping formulations at the center of the basemat are presented in Figure 11. The mean peak responses are presented in Table 6 and Table 7. The isolation level horizontal displacements using modal damping are significantly smaller than those obtained using the Rayleigh and Region options. The mean peak spectral accelerations obtained using the three options are comparable. The Rayleigh damping with *region* command has a more rational basis and is closer to a physically realistic mechanism in which different damping values are assigned to the isolation system and the superstructure.

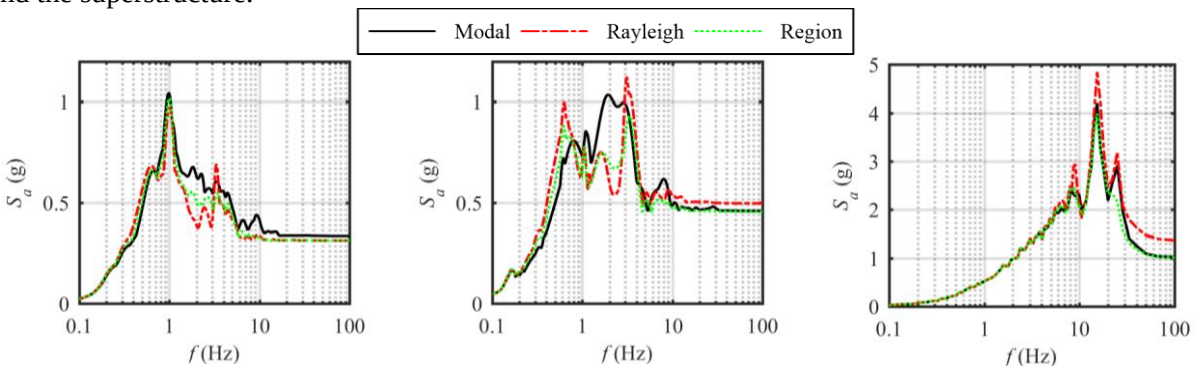

a) X direction b) Y direction c) Z direction

Figure 11. In-structure response spectra at the center of the basemat (2137)

Table 6. Mean peak in-structure response at the basemat of the LMS model for different formulations

No.	Damping	Resultant acc. (*g*)	Resultant disp. (mm)	Zero period acceleration (*g*)			Spectral acceleration (*g*)		
				a_X	a_Y	a_Z	S_{aX}	S_{aY}	S_{aZ}
I	Modal	0.37	158	0.30	0.33	1.05	1.05	1.09	3.83
II	Rayleigh	0.38	248	0.31	0.33	1.1	1.05	1.04	4.32
III	Region	0.35	206	0.28	0.3	0.99	1.02	0.96	3.54

Table 7. Mean peak in-structure response at the ASB of the LMS model for different formulations

No.	Damping	Resultant acc. (*g*)	Resultant disp. (mm)	zero period acceleration (*g*)			spectral acceleration (*g*)		
				a_X	a_Y	a_Z	S_{aX}	S_{aY}	S_{aZ}
I	Modal	0.39	159	0.31	0.35	1.44	1.06	1.10	5.94
II	Rayleigh	0.39	249	0.31	0.34	1.48	1.06	1.05	6.16
III	Region	0.35	207	0.29	0.31	1.29	1.02	0.97	4.72

LS-DYNA

Damping models are implemented in LS-DYNA at the element level. The global stiffness matrix is not formed in explicit analysis. The internal forces are obtained by integrating stresses over the element area and the Rayleigh damping terms are added as correction to these stresses (LSTC, 2016).

The damping formulations available in LS-DYNA are summarized in Table 8. A frequency-independent damping model, similar to modal damping, is available in LS-DYNA that assigns a damping value to a range of frequencies to a part set. This damping method is accurate only for small values of damping (1% to 2%) and the frequency range specified by the user should be within 30 (this ratio has been increased up to 100 from LS-DYNA ver 10). The achieved damping outside the range is smaller than the target damping. Mass proportional and stiffness proportional damping are available in LS-DYNA. Rayleigh damping can be used by assigning both the mass and stiffness proportional damping with appropriate coefficients. There

are two options for stiffness proportional damping in LS-DYNA: 1) Rayleigh coefficients (β_K) with negative sign follows the conventional formulation described previously, and 2) a positive value uniformly damps all the high frequency modes (LSTC, 2016). The details of the second option in the stiffness proportional damping is proprietary and not described in the LS-DYNA manuals.

Table 8. Damping options in LS-DYNA

Damping definition	LS-DYNA keyword
Uniform frequency range	*DAMPING_FREQUENCY_RANGE
Rayleigh	*DAMPING_PART_MASS + *DAMPING_STIFFNESS
Mass proportional	*DAMPING_GLOBAL, *DAMPING_PART_MASS
Stiffness proportional	*DAMPING_STIFFNESS

The uniform frequency damping, mass and the stiffness-proportional (and hence the Rayleigh) damping cannot be applied to discrete elements (LSTC, 2017). This was confirmed by assigning different values of damping to the isolation system with frequency range and stiffness proportional damping formulations and obtaining the response at the center of basemat. Results are plotted in Figure 12 and Figure 13. The isolator material in LS-DYNA (*MAT_ISOLATOR) has a parameter DAMP that specifies damping to the free axial vibration mode of the isolator based on the isolator mass and any other lumped masses. The default value of zero assigns a very high damping (100%) and limits any vertical amplification of the response, which is physically unrealistic. The plots of the in-structure response spectra were obtained with different values of the DAMP parameter and no significant effect was observed. No feasible option is available in LS-DYNA to assign damping to the vertical isolator response. A nominal value of DAMP=2% is recommended instead of default value of zero.

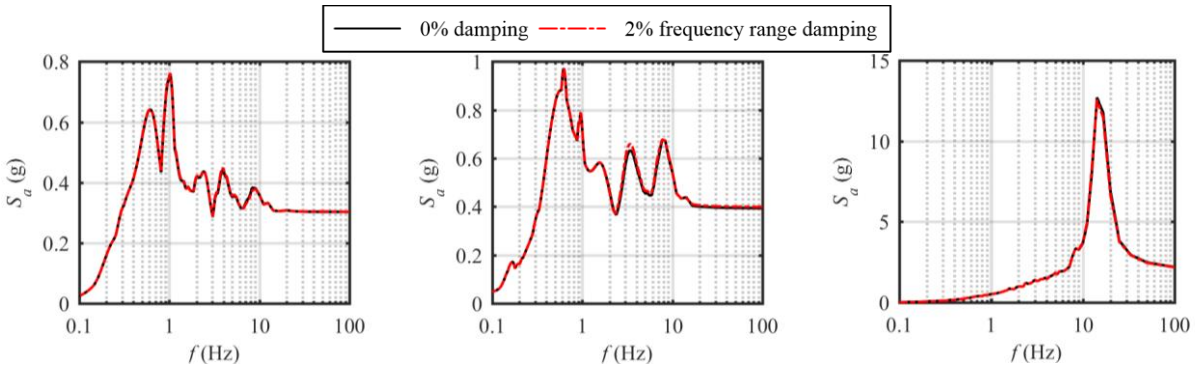

a) X direction b) Y direction c) Z direction

Figure 12. In-structure response spectra obtained using frequency range damping to the isolators

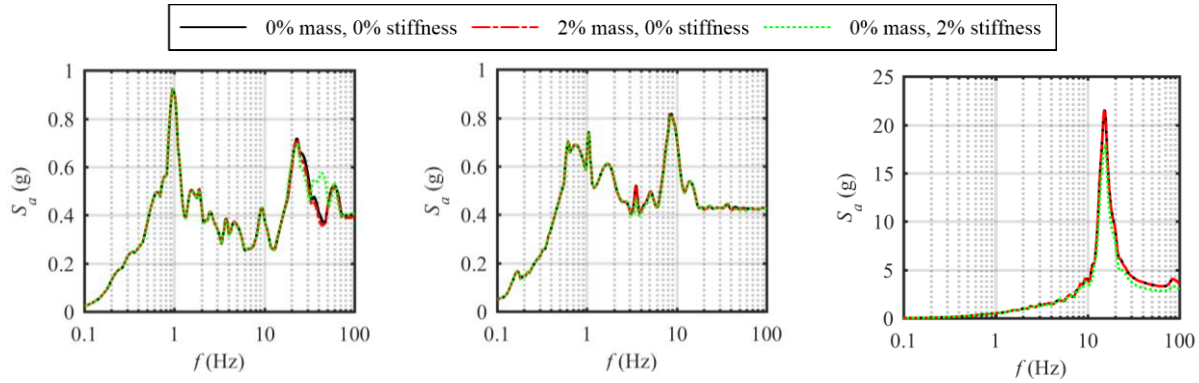

a) X direction b) Y direction a) Z direction

Figure 13. In-structure response spectra obtained using stiffness proportional damping for the isolators

LS-DYNA provides an option to assign values of damping to different parts of a FE model. This is similar to the *region* option available in OpenSees. Different parts can be assigned damping using any combination of available damping models in Table 8. Three damping strategies, summarized in Table 9, were implemented for the FE model of the base-isolated NPP. The traditional stiffness damping formulation is prone to convergence errors in LS-DYNA. The analysis using the Rayleigh damping as combination of mass and stiffness damping was terminating with a *negative volume* error. So, a modified Rayleigh damping formulation was used as the first damping definition (I) for the superstructure and the isolators. The superstructure was assigned a mass damping of 4% based on its first horizontal frequency and a damping of 4% using a stiffness damping formulation defined in LS-DYNA that uniformly damps all the high frequency modes (LSTC, 2016). For the second damping definition (II), uniform frequency range damping of 4% and 2% were used for the superstructure and the isolators, respectively. The third damping option (III) uses a mixed formulation that defines modified damping approach I for the superstructure and the isolators are assigned mass proportional damping corresponding to the isolation frequency in addition to setting the parameter DAMP=0.02 for the axial vibration. The damping assigned to isolators supplemented the hysteretic damping provided by the LR bearings due to energy dissipation in the lead cores.

Table 9. Damping definitions used for the FE model in LS-DYNA

No.	Damping	Description	Superstructure	Isolators
I	Modified Rayleigh	Combination of mass proportional damping that damps lower modes and a LS-DYNA specific (proprietary) stiffness formulation that uniformly damps high frequency modes.	4%	2%
II	Uniform frequency	Equal damping to a frequency range of a part set.	4%	2%
III	Mixed formulation	Modified Rayleigh for superstructure and mass proportional damping to horizontal isolation mode and DAMP parameter in *MAT_ISOLATOR.	4%	2%

The in-structure response spectra at the center of the basemat using the damping formulations are presented in Figure 14. The modified Rayleigh and mixed formulation provides smaller horizontal spectral accelerations at lower frequencies (<1 Hz) and greater values at higher frequencies (>10 Hz) compared to the uniform frequency formulation. The uniform frequency damping provides smaller vertical accelerations at higher frequencies (>10 Hz). This can be attributed to the characteristics of each damping option previously described. The uniform damping formulation provides the target damping only up to 2% for the superstructure, which is smaller than 4% damping provided by the modified Rayleigh and mixed damping formulations. Stiffness proportional damping cannot be used to assign damping to the high frequency axial vibration of the isolators. Hence, the modified Rayleigh and mixed damping formulations result in large vertical accelerations.

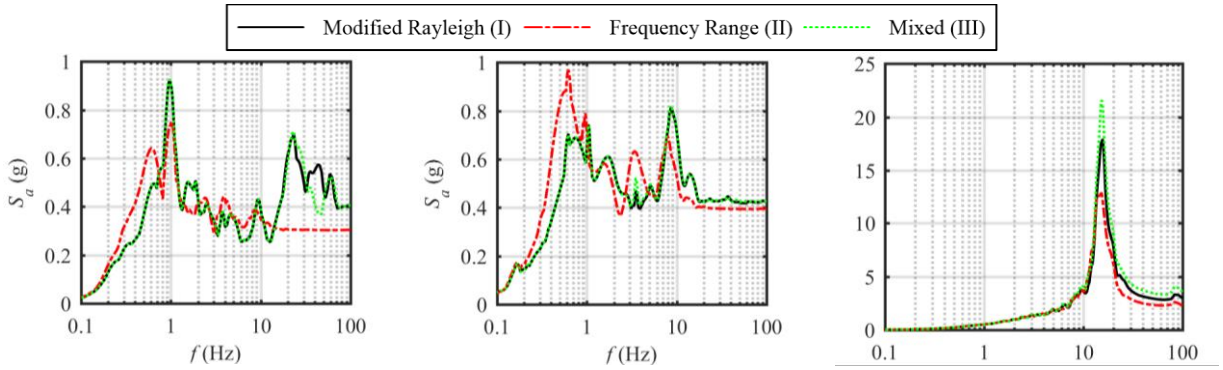

a) X direction b) Y direction b) Z direction

Figure 14. Floor response spectra obtained using different damping formulations

The lack of a feasible supplementary damping option to discrete isolator element is the biggest limitation of the FE model. This would have limited effect on the horizontal response of the isolation system where most of the damping is contributed by hysteretic energy dissipation in the lead-core of the LR bearing, but would significantly affect the vertical response and vertical in-structure spectra. The modified (I) and mixed (III) damping formulations provide the best solution in LS-DYNA to obtain horizontal displacement and in-structure acceleration response.

SUMMARY AND CONCLUSIONS

The accurate estimation of in-structure response of base-isolated NPPs is critical to the analysis and design of safety-related structural components. Damping models and their implementation in contemporary software programs significantly affect the response of a nonlinear system. There are unique challenges associated with the implementation of damping in a base-isolated structure due to the broad frequency range of interest and the markedly different damping characteristics of the isolators and the superstructure. Different damping formulations, and combinations thereof, were investigated to establish reasonable damping definitions for each of NPP model (i.e., TNM, LMS and FE) in OpenSees and LS-DYNA. The limitations of each damping formulation were also investigated. The key conclusions are presented below:

1. The modal, Rayleigh, mass and stiffness proportional damping formulations provide similar estimate of the horizontal isolator displacements.
2. The modal and mass proportional damping formulations underpredict vertical displacements and acceleration of the isolation system compared to the Rayleigh and stiffness proportional displacement.
3. The modal damping option in OpenSees cannot be applied to the TNM model of a base-isolated NPP.
4. The number of modes included in the modal damping definition to the LMS model in OpenSees affects the acceleration response at high frequency, especially in the axial direction.
5. The mass proportional damping should be only be used to assign damping to low frequency modes. For high frequency modes, stiffness and the Rayleigh damping provide response that is more realistic.
6. The Rayleigh damping with the region command provide a more rational basis for damping than the other options in OpenSees.
7. Supplemental damping cannot be applied to discrete isolators in LS-DYNA.
8. The use of the DAMP parameter in the isolator material in LS-DYNA is to ensure numerical stability and cannot be used to accurately estimate the vertical response of the isolation system.
9. There is high uncertainty associated with response at very high frequencies (>20 Hz) obtained using the damping options available in contemporary software programs. The vertical axial response cannot be obtained reliably with any of the available damping methods.

The assignment of damping plays a major role in the amplitude of the in-structure response of a base-isolated nuclear structure. The acceleration response, especially at high frequency, is more sensitive to the choice of damping than the displacement response. Experimental validation of alternate damping formulations might be required to estimate the in-structure response of base-isolated nuclear structures.

ACKNOWLEDGEMENT

The initial support for this research project was provided by the United States Nuclear Regulatory Commission (USNRC) through a grant to MCEER via a contract led by Dr. Robert Budnitz at the Lawrence Berkeley National Laboratory (LBNL). The authors acknowledge the important technical contributions of the Dr. Budnitz, the LBNL review panel, and Dr. Jose Pires of the USNRC to this research project. The latter part of the work presented in this paper was completed at IIT Bombay, which provided travel support to the lead author of this paper.

REFERENCES

Charney, F. A. (2008). "Unintended consequences of modeling damping in structures." *Journal of Structural Engineering*, 134(4), 581-592.
Chopra, A. K., and McKenna, F. (2015). "Modeling viscous damping in nonlinear response history analysis of buildings for earthquake excitation." *Earthquake Engineering & Structural Dynamics*, 193–211.
Computer & Structures Inc. (CSI) (2007). "SAP2000 user's manual–version 11.0." Berkeley, CA.
Electric Power Research Institute (EPRI). (2007). "Program on technology innovation: validation of CLASSI and SASSI codes to treat seismic wave incoherence in soil-structure interaction (SSI) analysis of nuclear power plant structures." *EPRI Technical Report 1015111*, Palo Alto, CA.
Hall, J. F. (1999). "Paper discussion: The role of damping in seismic isolation." *Earthquake Engineering & Structural Dynamics*, 28(12), 1717-1720.
Hall, J. F. (2006). "Problems encountered from the use (or misuse) of Rayleigh damping." *Earthquake Engineering & Structural Dynamics*, 35(5), 525-545.
Jehel, P., Léger, P., and Ibrahimbegovic, A. (2014). "Initial versus tangent stiffness-based Rayleigh damping in inelastic time history seismic analyses." *Earthquake Engineering & Structural Dynamics*, 43(3), 467-484.
Kelly, J. M. (1999). "The role of damping in seismic isolation." *Earthquake Engineering & Structural Dynamics*, 28(1), 3-20.
Kelly, J. M., and Marsico, M. R. (2015). "The influence of damping on floor spectra in seismic isolated nuclear structures." *Structural Control and Health Monitoring*, 22(4), 743-756.
Kumar, M., Whittaker, A., and Constantinou, M. (2014). "An advanced numerical model of elastomeric seismic isolation bearings." *Earthquake Engineering and Structural Dynamics*, 43(13), 1955-1974.
Kumar, M., Whittaker, A., and Constantinou, M. (2015a). "Experimental investigation of cavitation in elastomeric seismic isolation bearings." *Engineering Structures*, 101, 290-305.
Kumar, M., Whittaker, A., and Constantinou, M. (2015b). "Response of base-isolated nuclear structures to extreme earthquake shaking." *Nuclear Engineering and Design*, 295, 860–874.
Kumar, M., Whittaker, A., and Constantinou, M. (2015c). "Characterizing friction in sliding isolation bearings." *Earthquake Engineering & Structural Dynamics*, 44(9), 1409-1425.
Kumar, M., Whittaker, A. S., and Constantinou, M. C. (2015d). "Seismic isolation of nuclear power plants using elastomeric bearings." Technical Report MCEER-15-0008, University at Buffalo, State University of New York, Buffalo, NY.
Kumar, M., Whittaker, A. S., and Constantinou, M. C. (2015e). "Seismic isolation of nuclear power plants using sliding bearings." Technical Report MCEER-15-0006, University at Buffalo, State University of New York, Buffalo, NY.
Kumar, M., and Whittaker, A. (2018). "Cross-platform implementation, verification and validation of advanced mathematical models of elastomeric seismic isolation bearings." *Engineering Structures*, 175, 926-943.
Kumar, M., Whittaker, A. S., and Constantinou, M. C. (2019). "Seismic isolation of nuclear power plants using elastomeric bearing." NUREG/CR-7255, United States Nuclear Regulatory Commission, Washington, DC.
Léger, P., and Dussault, S. (1992). "Seismic energy dissipation in MDOF structures." *Journal of Structural Engineering*, 118(5), 1251-1269.
Livermore Software Technology Corporation (LSTC) (2016). "Damping in LS-DYNA." <http://www.dynasupport.com/howtos/general/damping>. (November 1, 2016).
LSTC (2017). "LS-DYNA keyword user's manual." Livermore Software Technology Corporation, Livermore, CA.
McKenna, F., Fenves, G., and Scott, M. (2006). Computer Program OpenSees: Open System for Earthquake Engineering Simulation, Pacific Earthquake Engineering Research Center, University of California, Berkeley, CA,(http://opensees.berkeley.edu).
Orr, R. (2003). "AP1000 inputs for 2D SASSI analyses." Edition, Westinghouse Electric Company, Cranberry Township, PA.
Petrini, L., Maggi, C., Priestley, M. J. N., and Calvi, G. M. (2008). "Experimental verification of viscous damping modeling for inelastic time history analysis." *Journal of Earthquake Engineering*, 12(sup1), 125-145.